Liquid Crystal ordering of DNA Dickerson Dodecamer duplexes with different 5'- Phosphate terminations

Marco Todisco[1], Gregory P. Smith[2], Tommaso P. Fraccia[3]

1 - *Dipartimento di Biotecnologie Mediche e Medicina Traslazionale, Università degli Studi di Milano, via Fratelli Cervi 93, I-20090 Segrate (MI), Italy*

2 - *Department of Physics and Soft Materials Research Center, University of Colorado, Boulder, CO, 80309-0390*

3 – Institute Pierre-Gilles de Gennes, ESPCI Paris, PSL Research University, 6 rue Jean Calvin, 75005 Paris, France

ABSTRACT

The onset of liquid crystal (LC) phases in concentrated aqueous solutions of DNA oligomers crucially depends on the end-to-end interaction between the DNA duplexes, which can be provided by the aromatic stacking of the terminal base-pairs or by the pairing of complementary dangling-ends. Here we investigated the LC behavior of three blunt-end 12-base-long DNA duplexes synthesized with hydroxyl, phosphate and triphosphate 5'-termini. We experimentally characterized the concentration-temperature phase diagrams and we quantitatively estimated the end-to-end stacking free energy, by comparing the empirical data with the predictions of coarse-grained linear aggregation models.

The preservation of LC ordering, even in presence of the bulky and highly charged triphosphate group, indicates that attractive stacking interactions are still preset and capable of induce linear aggregation of the DNA duplexes. This finding strengthens the potential role of chromonic like self-assembly for the prebiotic formation of linear polymeric nucleic acids.

INTRODUCTION

Liquid crystal (LC) ordering of concentrated aqueous solutions of DNA and RNA oligomers has been widely investigated in the recent years [1-12]. The formation of cholesteric, N*, and columnar, COL, LC phases of long nucleic acids, i.e. longer than 100 base pairs (bp), was discovered in the 90s by Livolant and coworkers [13,14], and it is a direct consequence of DNA double helix shape anisotropy and rigidity. Indeed, since DNA persistence length is 50 nm, i.e. of the order of 150 bp [15], polymeric DNA duplexes are surely hard rod-like molecules, which

satisfy the Onsager's constraint for liquid crystallization [16]. In the oligomeric regime (<20 bp), which is characterized by helical fragments whose length, $L < 6.8$ nm, is comparable to the diameter, $D = 2$ nm, the onset of LC phases takes place as consequence of the formation of physical reversible linear aggregates, overcoming the otherwise unsatisfied Onsager's rule of $L/D > 4$ [16]. Here, the key factor is the end-to-end interaction of short DNA duplexes, 6 to 20 bp, which can happen through the stacking of the terminal bases of blunt-end duplexes [1,2] or by pairing of complementary terminal dangling ends [5], which therefore become "sticky-ends". LC ordering has been extended to DNA sequences whose length doesn't permit double helix stability at room temperature, such as DNA 4mers [9,10]. Here the key factor is the simultaneous pairing and chaining of nicked strands which stabilizes the whole aggregates self-assembly. Even more surprising is the recently reported discovery that single bases DNA and RNA nucleotides (dNTPs and rNTPs) can give rise to COL phase when brought to high concentration and low temperature [4]. Being such monomeric level the minimal nucleic acids based system capable of pairing and stacking, it indicates that the formation of LC phases is a ubiquitous property of nucleic acids, regardless of the presence of the sugar-phosphate backbone [17]. Despite the several hydrogen bonding motifs which are accessible to canonical nucleobases, this happens only when the Watson-Crick pairing rule is satisfied, i.e. only if A-T or G-C pairing is possible [4]. In this latter case the nucleotides have 5' - triphosphate group, which plays the essential role of enhancing monomers solubility, even if such effect is still to be investigated more deeply.

The richness and robustness of oligo DNA and RNA LC phase phenomenology recently inspired the idea that it could have played a role for the prebiotic formation of polymeric nucleic acids [18]. Indeed, the self-assembly steps involved in this phenomenon can be seen as a process to enhance the formation of linear molecular products, which takes its foundation from the shape and interaction asymmetry of the involved building blocks. Which is lastly a propagation of the symmetry breaking derived by the properties of hydrogen bonding and stacking of aromatic nucleobases. In this frame, the onset of LC ordering of DNA and RNA oligomers, between 6 and 14 base-pairs long, is capable to boost the rate of non-enzymatic ligation reaction, increasing both reaction yield and product length, and favoring linear products against circular ones [19–21]. This process which has been named "LC autocatalysis" could have played a crucial role in series of events that brought to the origin of life on our planet [22].

The ligation of DNA or RNA strands requires the presence of a phosphate group at 5'- (or 3'-) termini, which must bind to a 3'- (or 5'-) hydroxyl termini of another strand. Normally this

reaction does not happen spontaneously, since the opposite process, the phosphodiester bond hydrolysis, is favored in aqueous environments, unless the ligation rate is enhanced by the coupling of some molecular moieties which work as good leaving groups. Water soluble carbodiimides, as EDC or CDI, are the most efficient phosphate activating agents [23,24]. Imidazole compounds are good leaving groups too, with a reasonable prebiotic availability [25]. The breaking of a triphosphate group, with the production of pyrophosphate as leaving group, is the strategy adopted to produce phosphodiester bonds by the modern enzymes, such as ligases or polymerases. Despite triphosphate ligation is fairly ineffective in absence of the catalyzing enzymes or a templating strand [26,27], it could have provided a simple and straightforward prebiotic ligation strategy. Given the crucial role of phosphate termini for chemical reactions and the lack of a deep understanding of the way different phosphate termini perturbate the stacking of DNA duplexes, we carried a systematic study of the effect of three different 5' termini on the formation of liquid crystal phases. In particular, we investigated the LC behavior of the already well characterized Dickerson Dodecamer [1,4,28–30], in the presence of three different 5'- molecular terminations: 1) 5'- OH group, i.e. the standard DD duplex with no terminal phosphates; 2) 5'– single phosphate group (5'-P), i.e. the 5'-phosphorylated DD duplex, named pDD; 3) 5'– triphosphate group (5'-PPP), i.e. the 5'-triphosphorylated DD duplex, named 3pDD. We experimentally characterized the concentration, c_{DNA}, vs. temperature, T, phase diagram of these three systems and we quantitatively estimated the end-to-end stacking free energy, by comparing empirical data with the predictions of coarse-grained linear aggregation models in which DNA helices are simplified as sticky cylinders [31,32].

SYNTHESIS AND PURIFICATION

While the synthesis of DNA/RNA oligomers with OH termini or with 3' or 5' single phosphate modification is standard nowadays and can be easily obtained from the major nucleic acids producing companies, the synthesis of 5'-triphosphate oligomers is not so usual and commercially available. Therefore, we decided to synthesize by ourselves all the DNA sequences involved in this work. The synthesis of 5'-hydroxil Dickerson Dodecamer (DD, 5'-CGCGAATTCGCG-3'), 5'-phosphate (pDD, 5'-pCGCGAATTCGCG-3') and 5'-triphosphate (3pDD, 5'-pppCGCGAATTCGCG-3'), were executed using an Äkta Oligopilot by Amersham Pharmacia Biotech. Standard solid support approach was followed to obtain both DD and pDD. Triphosphorylation on the 5'-terminus of DD was achieved following a modified protocol from [33]. Oligos were phosphitylated directly on the synthesizer using one column volume of 2-

chloro-4H-1,3,2-benzodioxaphosphorin-4-one (1M solution of 1:4 dioxane to pyridine) followed by reaction with tributyammonium pyrophosphate (0.5M solution of 1:1 acetonitrile to pyridine). Both mixtures were protected by air oxidation working under Argon flux. The reactions were injected directly into the column and recycled for ~ 20 minutes to reach reaction completion. Column content was recovered, and DNA molecules were detached from the solid support by stirring for 8 hours the in 40ml of NH_4OH solution (28 ~ 30% w/w) in a sand bath at 50°C. In order to get rid of the beads, the suspension was cooled down to room temperature and vacuum filtered over a coarse frit.

The filtered solution was stripped of solvent under vacuum using a Heidolph rotory evaporator. Final volume was reduced to ~10ml. RP-HPLC was performed through a prep scale SepaxGP-C8 column (Sepax Technologies Inc) on a dual Varian Prostar 218 system tied to a Prostar 318 detector to yield purified 3pDD. The analyte was eluted with a linear gradient using 50 mM TEAA pH 7.0 as the primary buffer and Methanol as the secondary buffer.

The RP-HPLC elution fractions were characterized through MALDI experiments on a AB/Sciex Voyager DE-STR instrument. Samples from the collected fractions were serially diluted and spotted on the MALDI plate using 3-hydroxypicolinic acid as a matrix. We could confirm that 3pDD was present in the first eluted peak, with a retention time between 30 and 32 minutes. Analysis of chromatograph reveals an efficiency for the triphosphorilation reaction close to 5%.

3pDD fractions were pooled and salt-precipitated adding a NaCl (final concentration equal to 400mM) and an approximately equal volume of isopropanol. Precipitation was performed with centrifugation at 15’000g and 25°C for 10 minutes. Pellet was resuspended in 2ml 70% ethanol solution. The resulting solution was centrifuged at 15’000g and 25°C for 10 minutes. The pellet was air-dried at 37°C and the remaining pellet was resuspended in 2ml of milliQ water and lyophilized.

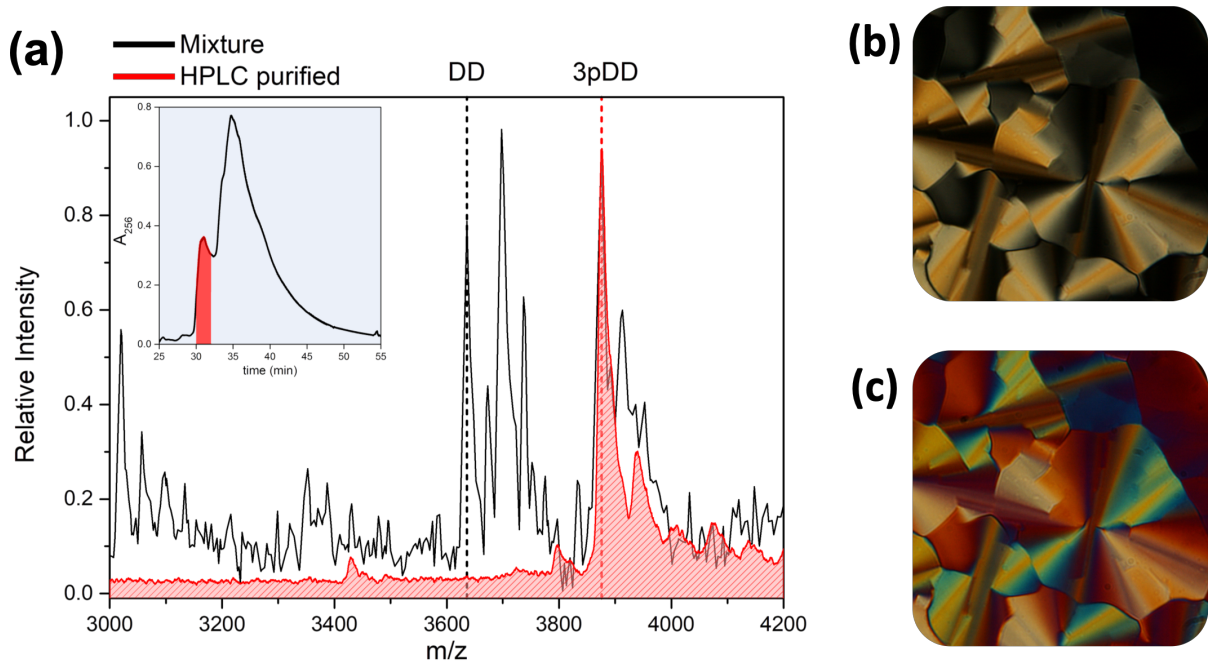

Figure 1. Synthesis and purification of 3pDD. (a) MALDI-TOF spectra of unpurified 3pDD synthesis product (black line) and after HPLC purification (red line). Elution peak corresponding to 3pDD is highlighted in red in the chromatograph (inlet). (b, c) Purified 3pDD readily produces liquid crystalline phases at high concentration, showing columnar focal conic textures observable through polarized transmitted optical microscopy (b) and with the addition of quarter-wave plate compensator (c). The combined observation of micrographs b and c allow to estimate a negative Δn for 3pDD, which is the same as for pDD and DD DNA oligos. This suggesting that the same ordering mechanism is at the basis of LC phases appearance.

RESULTS AND DISCUSSION

Characterization of 3pDD liquid crystal phases

To investigate the formation of LC phases for 3pDD duplexes, we produced glass planar microscope cells on which 1 µl drops were deposited, from a stock solution prepared at c_{DNA} = 50 mg/ml, and then let to dry. When LC phases appeared, the cells were covered with a second glass, glued and sealed with fluorinated oil, Fomblin Y25 Solvay, to prevent evaporation. Cell thickness of 20 µm between glass plates was guaranteed by silica rods spacers.

Fig. 1b,c and Fig. 2 show that 3pDD exhibits typical N* and COL textures. In particular, the analysis of columnar focal conics with a quarter-wave plate compensator, see Fig. 1b,c, shows that Δn is negative, as in the case for all DNA LC phases. The observation of the cholesteric textures reveals that the pitch, i.e. the periodicity of the twisted cholesteric planes along the direction perpendicular to the planes themselves, is in the micrometer range, Fig. 2a. The measurement of the pitch in the range between 0°C and 10°C shows that the pitch slightly increases with temperature, see graph in Fig. 2a. This behavior is the same previously observed

for DD N*, while surprisingly pDD was reported to have a pitch decreasing with T [7]. It has to be taken into account that more recently also DD pitch has been reported to decrease with temperature [29]. The disagreement between different measurements of the pitch for the same molecule can be explained by the different purification grade of the DNA oligomers, which can cause huge differences of ionic strength, prevalently due to Na^+ ions, and pH [9]. Both ionic strength and pH can tune the electrostatic repulsion between the charged backbone of the DNA duplexes, having effect on the final twist between neighboring molecules.

The handedness of the cholesteric phase can be determined by de-crossing the polarizers. As shown in Fig. 2b, the cholesteric domains having axes perpendicular to the cell plates, i.e. along the direction of observation, are bluish when observed between crossed polarizers, see central micrograph of Fig. 2a. The bluish color is due to selective reflection of the N* phase having the pitch in the infrared. The cholesteric domains can be extinguished only when the analyzer is de-crossed counter-clockwise, left micrograph, and not when it's rotated clockwise, right micrograph. This indicates that the N* phase of 3pDD is left-handed. This is quite surprising since both DD and pDD have been previously reported to display right-handed cholesterics [7]. This apparent contradiction can be explained once more by the different conditions in which the experiments were carried. Right-handed N* were observed in samples with ISO-N* transition, at 25°C, that was taking place at very high concentrations, c_{DNA} = 730 mg/ml for DD and c_{DNA} = 670 mg/ml for pDD in ref. [7] and c_{DNA} = 610 mg/ml for DD in ref. [29]. These values are more than the double of those observed here, see phase diagrams in Fig. 3, and this difference is almost surely due to the difference in the ionic strength and pH of the DNA solutions. The DNA sequences used here, after the HPLC purification, were dissolved in milliQ water at c_{DNA} = 5 mg/ml, and were dialyzed overnight in 1L of milliQ water and then in 1L of NaCl 50 mM, in order to achieve the same ionic strength condition.

The handedness of the N* phase is ruled by the balance between the steric interaction between DNA duplexes, which favors the propagation of the right-handedness of the natural enantiomer helix, and the electrostatic repulsion, which instead favors the opposite left-handed chirality [34,35]. The balance of these two interactions depends on the distance between DNA duplexes, and therefore on DNA concentration, the first prevailing at high c_{DNA} and the latter at low c_{DNA}. In this frame it's not surprising that the N* phase of 3pDD could be left-handed, since it is found at $c_{DNA} \approx 480$ mg/ml.

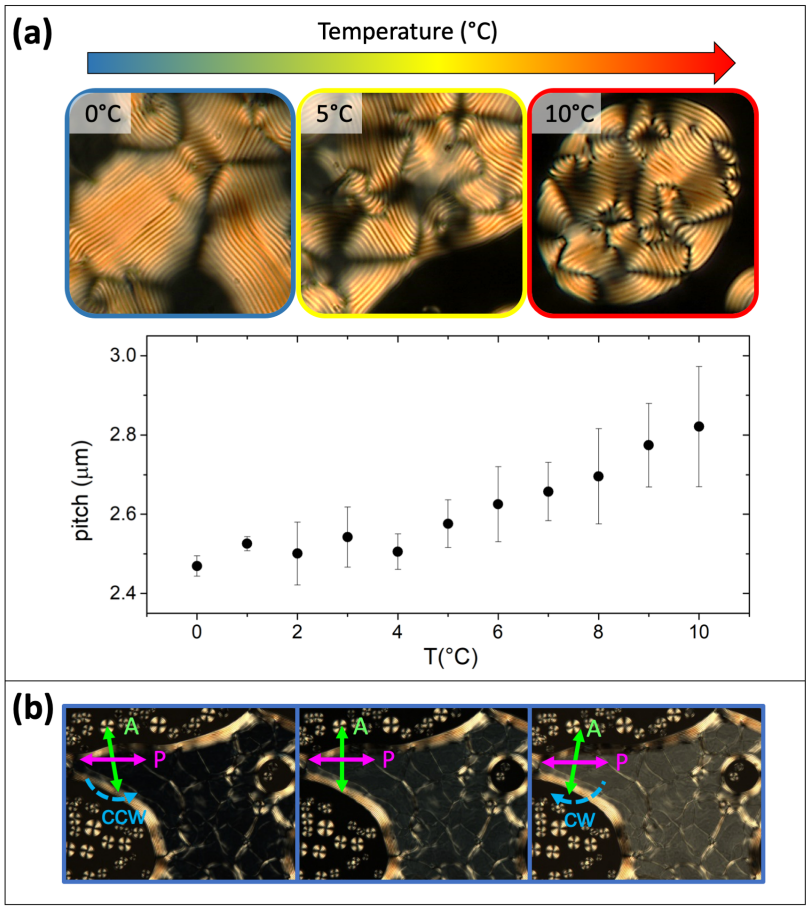

Figure 2. Characterization of cholesteric LC phases in 3pDD. (a,b) 3pDD can self-organize in cholesteric LC in a narrow range of concentrations ($c_{DNA} \approx 450$ - 500 mg/ml) with a pitch in the micrometer range. (a) The analysis of the periodicity of the characteristic fingerprints shows a positive dependence on temperature, *T*. (b) Transmitted light through cholesteric textures can be extinguished by rotating the analyzer counter-clockwise, indicating that the N* phase of 3pDD is left-handed.

Comparison of the phase diagrams of DD, pDD and 3pDD

The formation LC phases indicates that, even when the dodecamers are triphosphate terminated, there are attractive stacking interactions between the terminal nucleobases of blunt-ended duplexes. To assess the presence and strength of stacking interaction for DNA duplexes with the different 5'-phospate termination, we compared the phase behavior of aqueous solution of the dodecamers DD, pDD and 3pDD, which are sketched in the upper part of Fig. 3. Glass capillaries were also prepared by collecting 1 to 2 mg of lyophilized DNA powder, as measured with a 0.01 mg sensitivity scale, ABT 100-5M Kern, within a borosilicate capillary 0.5 mm diameter with a single pre-sealed end. By adding the desired volume of water with an Eppendorf P2.5 micropipette from the open end of the capillary and measuring the weight increase, we obtained a highly accurate method to investigate the phase diagram. The c_{DNA} vs. *T* phase diagrams for DD, pDD and 3pDD are shown in Fig. 3a,b,c, where the black, blue, red

and green symbols indicate the ISO, N*, COL and higher order columnar, C2, phases, respectively. Open symbols indicate the coexistence between isotropic and the LC phase, relative to the same color code. The comparison between the phase boundaries, reported in Fig. 3, clearly indicate that stacking interactions are weaker in 3pDD, since LC phases appear only at larger c and lower T, with respect to both DD and pDD. This appears reasonable given the larger electrostatic repulsion and of the bulkier terminal group provided by triphosphates.

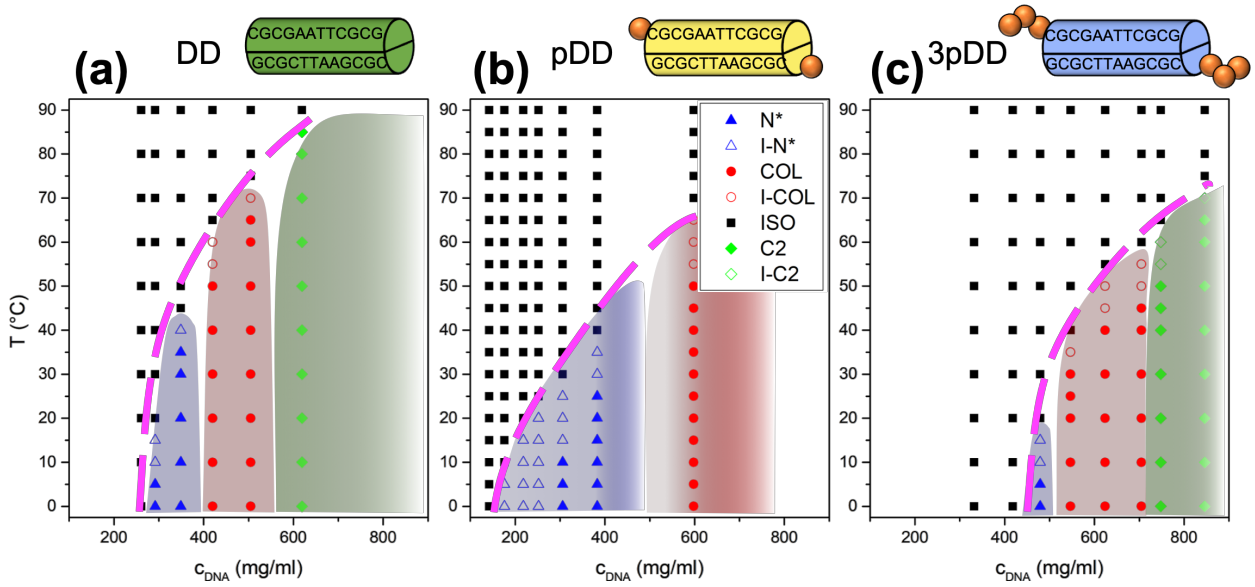

Figure 3. Supramolecular liquid crystal ordering in aqueous solutions of DD oligomers with different 5'-terminus functional groups. (a, b, c) Concentration, c_{DNA}, vs. temperature, T, phase diagrams of DD (a), pDD (b) and 3pDD (c) show that the presence of tri-phosphate groups at the 5'-terminus reduces the stability of the LC phases and increases the concentration required to undergo the liquid crystalline transition.

To quantitatively investigate the observed phase behavior, we used a coarse-grained model in which DNA duplexes are treated as hard cylinders with rounded edges that associate because of a square-well attractive interaction [31,32]. The terminal edges are decorated with a sticky semi sphere whose dimension indicates the range of the attractive potential. This model enables the calculation of the phase boundaries from geometrical and interaction parameters. In the isotropic phase, the cylinders aggregate forming chains of M monomers. The average aggregation number $\langle M \rangle$ depends on the ratio between the inter-monomer binding strength ΔG and the thermal energy $k_B T$ as

$$\langle M \rangle = \frac{1}{2}\left(1 + \sqrt{1 + 8\phi \frac{v_B}{v_D} e^{\Delta G / k_B T}}\right)$$

where ϕ is the volume fraction filled by cylinders, i.e. rescaled DNA concentration; v_B is the "bond volume", i.e. the volume that the center of mass of each cylinder can explore when part of an aggregate; v_D is the volume of a cylinder. According to the model the phase boundary marking the ISO side of ISO-LC coexistence is found when

$$\langle M \rangle \approx 0.75\, \phi^{-1.76} D/L$$

with D and L being the diameter and length of the cylinders, respectively. In the case of DD, pDD and 3pDD, $D/L \approx 0.5$, since $D = 2$ nm and $L = 12 \cdot 0.34$ nm = 4.08 nm. The volume fraction of DNA duplexes, ϕ, is obtained by assuming DNA density as 1687 g/l, as reported in ref. [4].

Recently, the stacking free energy ΔG between terminals of distinct bundles of DNA duplexes was evaluated experimentally [36]. The value obtained for CG/GC contacts of the kind involved in DD stacking, is about -2.15 kcal/mol, a value close to the one typically used for the same CG/GC contact in the nearest neighbor model for thermodynamic stability of DNA [37]. Another indirect evaluation of the stacking free energy ΔG for DD duplexes in LC phase, has been also obtained by exploiting the phase separation between the flexible polymer PEG and oligo DNA duplexes [11]. In this case, the comparison of the pressure, P, vs. c_{DNA} phase diagram, with the prediction of Montecarlo simulations from ref. [38], led to the estimation of $\Delta G \approx 6$ kcal/mol. Since the measurement in Ref. [36] does not provide the enthalpic, ΔH, and entropic, ΔS, contributions to ΔG separately, we decided to adopt those of the broadly adopted model of Ref. [37]: $\Delta H = -9.8$ kcal/mol and $\Delta S = -24.4$ cal / (mol K), or $\Delta G \sim 2$ kcal/mol.

These values, plus the geometrical parameters of the DD duplexes, are not sufficient to calculate the phase diagram. To compute $\langle M \rangle$ it is necessary to know the ratio v_B/v_D, a value which is very difficult to estimate without a detailed knowledge of the stacking potential. Moreover, having adopted in the calculation nearest neighbor values, which are obtained in the context of the internal interaction in chemically continuous double helices, the bond volume must also effectively include a correction for the entropy associated to the azimuthal freedom of the interacting duplexes.

To compare the values of ΔG for the stacking of duplexes with added phosphates with the value of the OH terminated duplexes, we varied both the interaction strength and the parameter v_B/v_D, to approximate the phase boundaries. Thus, we uniformly changed both enthalpy and entropy by a multiplicative factor A, which gives $\Delta H' = A \cdot \Delta H$ and $\Delta S' = A \cdot \Delta S$ and the parameter v_B/v_D in order to approximate the phase boundaries. The experimental ISO-LC phase boundaries and

their approximation from the coarse-grained model are reported in Fig. 4, as filled data points and straight lines, respectively.

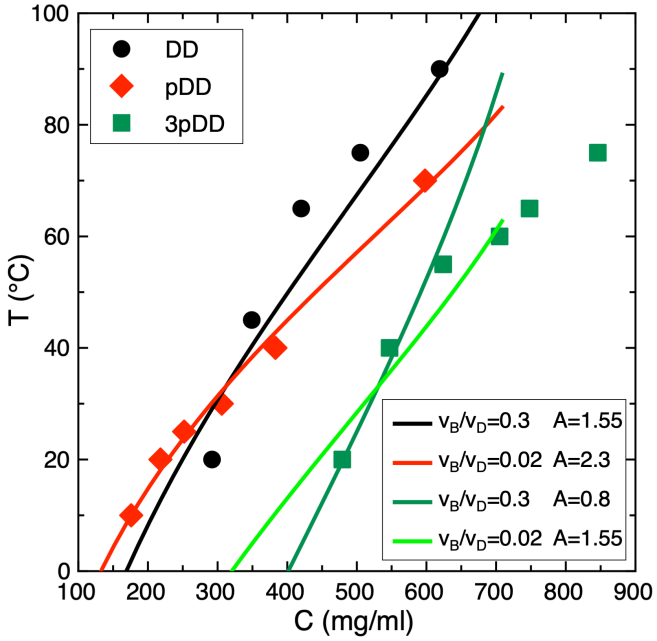

Figure 4. Comparison of the phase boundaries of DD, pDD and 3pDD with the prediction of the coarse-crained model. The experimental c_{DNA} and T data of the ISO-LC phase boundaries for DD, pDD and 3pDD are reported by the filled symbols, in black circles, red diamonds and green squares, respectively. The lines are the predicted phase boundaries from the coarse-grained model of ref. [31], that better approximate the experimental data. The simulation parameters v_B/v_D and A, which are reported in the legend, allow the calculation of the intermolecular end-to-end stacking free energy at 37°C for the three investigated DNA duplexes: ΔG_{DD} = 2.73 kcal/mol, ΔG_{pDD} = 2.74 kcal/mol, ΔG_{3pDD} = 1.05 kcal/mol for v_B/v_D = 0.3, and ΔG_{3pDD} = 1.07 kcal/mol for v_B/v_D = 0.02.

When A = 1.55 and v_B/v_D = 0.3 the phase boundary best matches the one of DD (black line in Fig. 4). To evaluate how much the stacking energy should be reduced to shift the DD phase boundary toward that of 3pDD, we proceeded via two different routes. First, we kept v_B/v_D = 0.3 fixed and reduced the energy. When A = 0.8 the phase boundary best matches the one of 3pDD (green line in Fig. 4). Second, since the presence of a terminal phosphate has been shown to stabilize the azimuthal freedom of the stacked duplexes [39], we held $\Delta G'$ as in DD and decreased the value of v_B/v_D. We find that when $v_B/v_D \approx 0.02$, the predicted phase boundary approximates that of 3pDD (green light line in Fig. 4). Finally, to match the phase boundaries of pDD, we kept the reduced v_B/v_D as found in 3pDD, and we uniformly changed enthalpy and entropy. When A = 2.2 the phase boundary best matches the one of pDD (red line in Fig. 4).

In order to compare the obtained stacking energies, we incorporated the reduced bond volume into the free energy value yielding: ΔG_{DD} = 2.73 kcal/mol, ΔG_{pDD} = 2.74 kcal/mol, ΔG_{3pDD} = 1.05 kcal/mol for v_B/v_D = 0.3, and ΔG_{3pDD} = 1.07 kcal/mol for the reduced v_B/v_D = 0.02, at 37°C. Thus, this analysis suggests that the free energy of stacking of triphosphate terminated duplexes is much lower of the one involved in non-phosphorylated duplexes, around 2.5 times. This can be explained by the reasonable entropic penalty given by the steric occupation of the triphosphate chains and the high electrostatic repulsion of such charged moieties. On the other hand, the addition of a single phosphate isn't affecting appreciably the interaction strength. This is in agreement with the results of atomistic simulations which show that the phosphate terminus enhances the azimuthal lockage of the interacting duplexes [39].

CONCLUSIONS

The LC phase diagrams of three version of the 12mer DNA sequence, 5'-CGCGAATTCGCG-3', with 5'-OH, 5'-P and 5'-PPP termini, have been investigated and quantitatively compared. Despite the potentially destabilizing variety of chemical modification of the 5'-termini, LC ordering is preserved in all cases. LC ordering of nucleic acids stabilizes the physical continuity of long double helixes formed by the aggregation of short duplexes despite the different chemical terminations. The persistence of LC phases in triphosphate terminated DNA duplexes strengthens the potential role of nucleic acids self-assembly in the context of the origin of life [18,22]. Thus, the reported results indicates that the mechanism of LC autocatalysis, that we previously suggested [19–21], is applicable even in the presence of bulky, charged and, importantly, potentially reactive terminal groups for the abiotic polymerization of nucleic acids.

AKNOWLEDGEMENT

We are indebted to Tommaso Bellini and Noel A. Clark for having incited this work, for the fundamental support for the calculation of the phase boundaries from the model and, most importantly, for having introduced us to the fascinating world of DNA liquid crystals. M.T. acknowledges the support of the Invernizzi Fundation.

M.T., G.P.S. and T.P.F. conceived the experiments; M.T. and G.P.S. performed the DNA synthesis; M.T., G.P.S. and T.P.F. performed the experiments; M.T. and T.P.F. analyzed the data; T.P.F. wrote the manuscript.

The authors declare that they have no competing interests.

REFERENCES

1. Nakata, M.; Zanchetta, G.; Chapman, B. D.; Jones, C. D.; Cross, J. O.; Pindak, R.; Bellini, T.; Clark, N. A. End-to-end stacking and liquid crystal condensation of 6 to 20 base pair DNA duplexes. *Science* **2007**, *318*, 1276–1279, doi:10.1126/science.1143826.
2. Zanchetta, G.; Bellini, T.; Nakata, M.; Clark, N. A. Physical polymerization and liquid crystallization of RNA oligomers. *J. Am. Chem. Soc.* **2008**, *130*, 12864–12865, doi:10.1021/ja804718c.
3. Lucchetti, L.; Fraccia, T. P.; Ciciulla, F.; Bellini, T. Non-linear optical measurement of the twist elastic constant in thermotropic and DNA lyotropic chiral nematics. *Sci. Rep.* **2017**, *7*, doi:10.1038/s41598-017-05136-z.
4. Smith, G. P.; Fraccia, T. P.; Todisco, M.; Zanchetta, G.; Zhu, C.; Hayden, E.; Bellini, T.; Clark, N. A. Backbone-free duplex-stacked monomer nucleic acids exhibiting Watson–Crick selectivity. *Proc. Natl. Acad. Sci.* **2018**, 201721369, doi:10.1073/pnas.1721369115.
5. Zanchetta, G.; Nakata, M.; Buscaglia, M.; Clark, N. A.; Bellini, T. Liquid crystal ordering of DNA and RNA oligomers with partially overlapping sequences. *J. Phys. Condens. Matter* **2008**, *20*, 494214, doi:10.1088/0953-8984/20/49/494214.
6. Zanchetta, G.; Nakata, M.; Buscaglia, M.; Bellini, T.; Clark, N. A. Phase separation and liquid crystallization of complementary sequences in mixtures of nanoDNA oligomers. *Proc. Natl. Acad. Sci. U. S. A.* **2008**, *105*, 1111–1117.
7. Zanchetta, G.; Giavazzi, F.; Nakata, M.; Buscaglia, M.; Cerbino, R.; Clark, N. a; Bellini, T. Right-handed double-helix ultrashort DNA yields chiral nematic phases with both right- and left-handed director twist. *Proc. Natl. Acad. Sci. U. S. A.* **2010**, *107*, 17497–17502, doi:10.1073/pnas.1011199107.
8. Bellini, T.; Zanchetta, G.; Fraccia, T. P.; Cerbino, R.; Tsai, E.; Smith, G. P. Liquid crystal self-assembly of random- sequence DNA oligomers. *Proc. Natl. Acad. Sci. U. S. A.* **2012**, *109*, 1110–1115, doi:10.1073/pnas.1117463109.
9. Fraccia, T. P.; Smith, G. P.; Bethge, L.; Zanchetta, G.; Nava, G.; Klussmann, S.; Clark, N. A.; Bellini, T. Liquid Crystal Ordering and Isotropic Gelation in Solutions of Four-Base-Long DNA Oligomers. *ACS Nano* **2016**, *10*, 8508−8516, doi:10.1021/acsnano.6b03622.
10. Fraccia, T. P.; Smith, G. P.; Clark, N. A.; Bellini, T. Liquid crystal ordering of four-

base-long DNA oligomers with both G–C and A–T pairing. *Crystals* **2018**, *8*, doi:10.3390/cryst8010005.

11. Di Leo, S.; Todisco, M.; Bellini, T.; Fraccia, T. P. Phase separations, liquid crystal ordering and molecular partitioning in mixtures of PEG and DNA oligomers. *Liq. Cryst.* **2018**, 1–13, doi:10.1080/02678292.2018.1519123.
12. Lucchetti, L.; Fraccia, T. P.; Ciciulla, F.; Simoni, F.; Bellini, T. Giant optical nonlinearity in DNA lyotropic liquid crystals. *Opt. Express* **2017**, *25*, doi:10.1364/OE.25.025951.
13. Livolant, F.; Levelut, A. M.; Doucet, J.; Benoit, J. P. The highly concentrated liquid-crystalline phase of DNA is columnar hexagonal. *Nature* **1989**, *339*, 724–726.
14. Leforestier, a; Livolant, F. Supramolecular ordering of DNA in the cholesteric liquid crystalline phase: an ultrastructural study. *Biophys. J.* **1993**, *65*, 56–72, doi:10.1016/S0006-3495(93)81063-4.
15. Lu, Y.; Weers, B.; Stellwagen, N. C. DNA persistence length revisited. *Biopolymers* **2001**, *61*, 261–275, doi:10.1002/bip.10151.
16. Onsager, L. The effects of shape on the interaction of colloidal particles. *Ann. N. Y. Acad. Sci.* **1949**, *51*, 627–659.
17. Podgornik, R. Sticking and stacking: Persistent ordering of fragmented DNA analogs. *Proc. Natl. Acad. Sci.* **2018**, *115*, 8652–8654, doi:10.1073/pnas.1810662115.
18. Budin, I.; Szostak, J. W. Expanding roles for diverse physical phenomena during the origin of life. *Annu. Rev. Biophys.* **2010**, *39*, 245–63, doi:10.1146/annurev.biophys.050708.133753.
19. Fraccia, T. P.; Smith, G. P.; Zanchetta, G.; Paraboschi, E.; Yi, Y.; Yi, Y.; Walba, D. M.; Dieci, G.; Clark, N. A.; Bellini, T. Abiotic ligation of DNA oligomers templated by their liquid crystal ordering. *Nat. Commun.* **2015**, *6*, 6424, doi:10.1038/ncomms7424.
20. Fraccia, T. P.; Zanchetta, G.; Rimoldi, V.; Clark, N. A.; Bellini, T. Evidence of Liquid Crystal–Assisted Abiotic Ligation of Nucleic Acids. *Orig. Life Evol. Biosph.* **2015**, *45*, doi:10.1007/s11084-015-9438-1.
21. Todisco, M.; Fraccia, T. P.; Smith, G. P.; Corno, A.; Bethge, L.; Klussmann, S.; Paraboschi, E. M.; Asselta, R.; Colombo, D.; Zanchetta, G.; Clark, N. A.; Bellini, T. Nonenzymatic Polymerization into Long Linear RNA Templated by Liquid Crystal Self-Assembly. *ACS Nano* **2018**, acsnano.8b05821, doi:10.1021/acsnano.8b05821.
22. Lazcano, A. Prebiotic Evolution and Self-Assembly of Nucleic Acids. *ACS Nano*

2018, acsnano.8b07605, doi:10.1021/acsnano.8b07605.

23. Dolinnaya, N. G.; Tsytovich, a V; Sergeev, V. N.; Oretskaya, T. S.; Shabarova, Z. a Structural and kinetic aspects of chemical reactions in DNA duplexes. Information on DNA local structure obtained from chemical ligation data. *Nucleic Acids Res.* **1991**, *19*, 3073–3080.
24. Shabarova, Z. A.; Merenkova, I. N.; Oretskaya, T. S.; Sokolova, N. I.; Skripkin, E. A.; Alexeyeva, E. V; Balakin, A. G.; Bogdanov, A. A. Chemical ligation of DNA: **1991**, *19*, 4247–4251.
25. Schrum, J. P.; Ricardo, A.; Krishnamurthy, M.; Blain, J. C.; Szostak, J. W. Efficient and rapid template-directed nucleic acid copying using 2'-amino-2',3'-dideoxyribonucleoside-5'- phosphorimidazolide monomers. *J. Am. Chem. Soc.* **2009**, *131*, 14560–14570.
26. Rohatgi, R.; Bartel, D. P.; Szostak, J. W. Kinetic and Mechanistic Analysis of Nonenzymatic , Template-Directed Oligoribonucleotide Ligation. **1996**, *9*, 3332–3339.
27. Rohatgi, R.; Bartel, D. P.; Szostak, J. W. Nonenzymatic , Template-Directed Ligation of Oligoribonucleotides Is Highly Regioselective for the Formation of 3 ′ - 5 ′ Phosphodiester Bonds. **1996**, 3340–3344, doi:10.1021/ja9537134.
28. Drsata, T.; Pérez, A.; Orozco, M.; Morozov, A. V.; Soner, J.; Lankas, F. Structure, stiffness and substates of the dickerson-drew dodecamer. *J. Chem. Theory Comput.* **2013**, *9*, 707–721.
29. De Michele, C.; Zanchetta, G.; Bellini, T.; Frezza, E.; Ferrarini, A. Hierarchical Propagation of Chirality through Reversible Polymerization: The Cholesteric Phase of DNA Oligomers. *ACS Macro Lett.* **2016**, *5*, 208–212, doi:10.1021/acsmacrolett.5b00579.
30. Rossi, M.; Zanchetta, G.; Klussmann, S.; Clark, N. a.; Bellini, T. Propagation of chirality in mixtures of natural and enantiomeric dna oligomers. *Phys. Rev. Lett.* **2013**, *110*, 107801, doi:10.1103/PhysRevLett.110.107801.
31. De Michele, C.; Bellini, T.; Sciortino, F. Self-assembly of bifunctional patchy particles with anisotropic shape into polymers chains: Theory, simulations, and experiments. *Macromolecules* **2012**, *45*, 1090–1106.
32. Nguyen, K. T.; Sciortino, F.; De Michele, C. Self-assembly-driven nematization. *Langmuir* **2014**, *30*, 4814–4819, doi:10.1021/la500127n.
33. Lebedev, A. V; Koukhareva, I. I.; Beck, T.; Vaghefi, M. M. Preparation of oligodeoxynucleotide 5′-triphosphates using solid support approach. *Nucleosides,*

Nucleotides and Nucleic Acids **2001**, *20*, 1403–1409, doi:10.1081/NCN-100002565.

34. Frezza, E.; Ferrarini, A.; Kolli, H. B.; Giacometti, A.; Cinacchi, G. The isotropic-to-nematic phase transition in hard helices: Theory and simulation. *J. Chem. Phys.* **2013**, *138*, 24, doi:10.1063/1.4802005.
35. Kolli, H. B.; Frezza, E.; Cinacchi, G.; Ferrarini, A.; Giacometti, A.; Hudson, T. S. Communication: From rods to helices: Evidence of a screw-like nematic phase. *J. Chem. Phys.* **2014**, *140*, 10–15, doi:10.1063/1.4866808.
36. Kilchherr, F.; Wachauf, C.; Pelz, B.; Rief, M.; Zacharias, M.; Dietz, H. Single-molecule dissection of stacking forces in DNA. *Science (80-.).* **2016**, *353*.
37. SantaLucia, J.; Hicks, D. The thermodynamics of DNA structural motifs. *Annu. Rev. Biophys. Biomol. Struct.* **2004**, *33*, 415–40, doi:10.1146/annurev.biophys.32.110601.141800.
38. Kuriabova, T.; Betterton, M. D.; Glaser, M. a. Linear aggregation and liquid-crystalline order: comparison of Monte Carlo simulation and analytic theory. *J. Mater. Chem.* **2010**, *20*, 10366, doi:10.1039/c0jm02355h.
39. Maffeo, C.; Luan, B.; Aksimentiev, A. End-to-end attraction of duplex DNA. *Nucleic Acids Res.* **2012**, *40*, 3812–3821.